Photoacoustic Tomography for Brain Imaging

Group Members:
IA
Mahri K

Assisted by:
University of Texas at Arlington, Department of Biomedical Engineering

Course Instructor:
Baohong Yuan

TA:
Yang Liu

December 13th, 2021

Contents

Introduction

Neuroimaging or brain scanning involves the use of various techniques to image the structure, function, or pharmacology of the brain directly or indirectly. Structural imaging of the brain deals with the structure of the brain and diagnosis of large-scale intracranial disease such as brain tumors. Functional imaging is used to diagnose metabolic diseases and lesions on a finer scale, like Alzheimer's disease. CT, fMRI, PET and SPET are most widely used imaging modalities for diagnostic structural and functional brain imaging. A fundamental constraint of these modalities is cost and spatial resolution.

Photoacoustic tomography (PAT) is an emerging imaging modality that provides non-invasive high-resolution images of the entire brain in a preclinical setting at near real time [5]. It is a hybrid imaging modality that combines rich optical contrasts with a high ultrasonic spatial resolution in deep tissue. PAT is based on the photoacoustic effect which starts with optical absorption by tissue molecules and ends with ultrasonic wave emission through thermoelastic expansion. Thus, PAT is known to offer two advantages over other imaging modalities, the resultant PA signal is sensitive to the rich optical absorption contrast of the biological tissue which allows for functional and metabolic imaging capabilities and the acoustic waves are less sensitive to scattering as light which leads to high spatial resolution in deep tissue and low procedure cost [14].

Principles and Experimental Setup

Photoacoustic tomography utilizes optical properties as well as acoustic properties of living tissues. PAT uses ultrasound imaging principles however, the acoustic wave is not generated by the transducer in PAT.

The principles of PAT include sending pulsed laser beam signals or electromagnetic wave signals to the area of interest for a duration of nanoseconds [11]. Irradiation of the area of interest by the pulsed laser beam creates the diffusion of the photons within the tissue of interest due to the nature of human tissues. This phenomenon can be observed after travelling about one transport mean free path (TMFP or l_t^1) which is typically ~1 mm in muscle and ~ 0.6 mm in the brain [11,14]. When these photons interact with the biological tissues, the molecule absorbs the photon energy and transitions from ground state to the excited state. This extra energy that was gained by the molecule will need to decay because the molecule is unstable when it possesses extra energy. Thus, this energy can decay in the form of radiative decay or thermal dissipation [7]. If the pulsed laser beam is a short pulse (time domain), or if it is the intensity modulated pulse (frequency domain), the generated heat during thermal dissipation produces photoacoustic waves via thermal expansion [8]. This thermal energy transformed to photoacoustic waves travels omni-directionally rather than toward a specific direction. Transducer positioned close to the area of imaging is used to detect the incoming acoustic wave signals from the target area.

Natural biological tissues are known to have strong scattering behavior, nevertheless, PAT imaging can achieve good spatial resolution to be able to provide effective data [12].

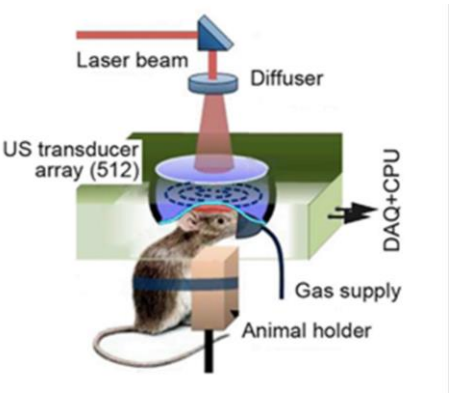

Figure 1: Schematic showing the working principle of the photoacoustic tomography imaging technique for the brain imaging of a mouse [2].

Pulsed laser beam heating involves two-time scales, thermal relaxation time and stress relaxation time [7]. Thermal relaxation is the thermal diffusion over a region, and it is equal to:

$$\tau_{th} = \frac{d_c^2}{\alpha_{th}}$$

where α_{th} represents the thermal diffusivity (m^2/s) and d_c represents characteristic dimension of the heated region or the desired spatial resolution [7].

The stress relaxation time is used to describe the pressure propagation:

$$\tau_s = \frac{d_c}{v_s}$$

where d_c is the characteristic dimension of the heated region, or the desired spatial resolution and v_s is the speed of sound (m/s) [7]. On some occasions the speed of sound in soft tissue can be considered constant, ~1.55 mm/ µs.

The volume expansion due to the excitation can be modeled as following:

$$\frac{dV}{V} = -\kappa p + \beta T$$

where κ is the isothermal compressibility (Pa^{-1}), β is the thermal coefficient of volume expansion (K^{-1}), p is the pressure (Pa), and T is temperature (K) [7].

In photoacoustic tomography procedure, the generation of the pressure difference is the crucial part in generating photoacoustic waves. Initial pressure distribution p_0 , which is known to be caused by the pulsed laser beam, is proportional to the product of the optical fluence and absorption coefficient of the point of interest. The absorption coefficient is different for every tissue. Optical fluence F(r) [J/cm2] is defined as the total number of photons passing through a unit of area over a period of time and at position (r) [13]. When the optical fluence is deeper than

one transport mean free path, the pulsed laser beam shows broad distribution. When optical fluency is considered to be uniform over an image area the absorption coefficient and the gross concentration of chromophores can be obtained by acquiring the spatial distribution data.

Initial pressure rise p_0 can be modeled by the following equations: $p_0 = \frac{\beta T}{\kappa}$, where β is the thermal coefficient of the volume expansion (K^{-1}), T is the temperature (K) and κ is the isothermal compressibility (Pa^{-1}) [7]. The above equation can be rewritten in the following way: $p_0 = \frac{\beta}{\kappa}\frac{\eta_{th} * A_e}{p * C_v}$, where β is the thermal coefficient of the volume expansion (K^{-1}), κ is the isothermal compressibility (Pa^{-1}) , is the specific optical absorption (J/m^3), is the percentage of absorbed energy that is converted to heat, p is the mass density (kg/m^3) and C_v is the specific heat capacity at constant volume (J/(kg*K)) [7]. Gruneisen parameter, Γ , can be used to simplify the initial pressure equation in the following way:

$$\Gamma = \frac{\beta}{\kappa * p * C_v}$$

$$p_0 = \Gamma * \eta_{th} * A_e$$

A_e , which is the specific optical absorption (J/m^3), is proportional to the local optical fluence F if the behavior exhibited by the tissue is of linear optical absorption represented by:

$$p_0 = \Gamma * \eta_{th} * \mu_a * F$$

where μ_a is the optical absorption coefficient (cm^{-1}) [7].

The instant pressure increase within the region of interest due to the deposit of laser energy gives rise to the thermal expansion effect to release the acquired pressure which consequently produces the ultrasonic wave, known as photoacoustic wave. The acoustic pressure p of the photoacoustic wave can be modeled by the wave equation that is utilized in the ultrasound imaging principles:

$$\left(\nabla^2 - \frac{1}{v_s^2} * \frac{\partial^2}{\partial t^2}\right) * p = -\frac{\beta}{C_p} * \frac{\partial H}{\partial t}$$

where H is the heating function defined as the heat deposited per unit volume and per unit time and it is related to the specific optical absorption, A_e , ∇^2 is the Laplace operator, v_s is the speed of sound (m/s), β is the thermal coefficient of the volume expansion (K^{-1}), C_p is the specific heat capacity at constant pressure [7]. The heating function can be further rewritten in the following way:

$$H(\underset{r}{\rightarrow}, t) = p * C_v * \frac{\partial T(\underset{r}{\rightarrow}, t)}{\partial t}$$

which can be combined with the wave equation above and using the Green function approach, we can solve the equations and obtain delta heating response in the following model:

$p_\delta(\vec{r}, t) = \frac{\partial}{4*\pi*v_s^2*\partial t}[\int d\vec{r} * \frac{p_0(\vec{r}')}{|\vec{r} - \vec{r}'|} * \partial(t - \frac{|\vec{r} - \vec{r}'|}{v_s})]$, where $p_0(\vec{r}')$ is the initial pressure at location $\vec{r}'$ [17].

It is worth mentioning that the frequency domain photoacoustic utilize the Fourier transformation methods and Helmholtz equation, but the specific equations will not be discussed in this paper.

When the tissue is complex or inhomogeneous, it becomes harder to receive effective signals back. The reason for that is because the deeper the pulsed laser beam travels into the tissue, the more paths are available for photons to scatter within. After generating the photoacoustic wave, this wave has more opportunities to attenuate which eventually will cause a loss of signal. This is the exact issue with brain imaging using photoacoustic tomography techniques. Considering these challenges, we can assume the diffusion theory.

When dealing with the large depths which have TMFP much bigger than 1 mm (ex: the brain), the following equation can describe the distribution of optical fluence in the semi-infinite homogeneous medium: $F(r) \propto \frac{e^{-\sqrt{3\mu_a(\mu_a+\mu_s)}*r}}{r}$ where r represents the location of optical fluence, F, and $\sqrt{3\mu_a(\mu_a + \mu_s)}$ represents μ_{eff} which is the effective attenuation coefficient of tissue. PAT imaging can resolve the locations of the photoacoustic signal sources, thus achieving efficient spatial resolution.

Various depths of the penetration of the laser beam constitute various regimes. There are three regimes that have been analyzed using photoacoustic tomography so far: quasi ballistic regime, quasi diffusive regime, and diffusive regime. Quasi ballistic regime PAT has an imaging depth less than 1 TMFP (~ <0.6 mm). Quasi diffusive regime PAT accounts for imaging depth more than 1 TMFP but less than 10 TMFP which is about 0.6-6 mm [15] . Diffusive regime PAT has TMFP higher than 10 (~> 6 mm) which makes it very useful for deep brain imaging.

Several methods of photoacoustic signal detection have been explained in the study done by Yang and Ghim. The first method involves usage of the single element transducer (focused or unfocused). This method is applied to avoid cumbersome image reconstruction processes like computed tomographic reconstruction (Fig.2(a)). When dealing with photoacoustic signals that are coming from deep tissues, this technique excludes all the signals that approach from off-axial points. This happens due to the curved surface of the ultrasound transducer. The ultrasound transducer determines the lateral resolution in this method which is inversely proportional to the product of the center frequency and acoustic numerical aperture (NA) [11].

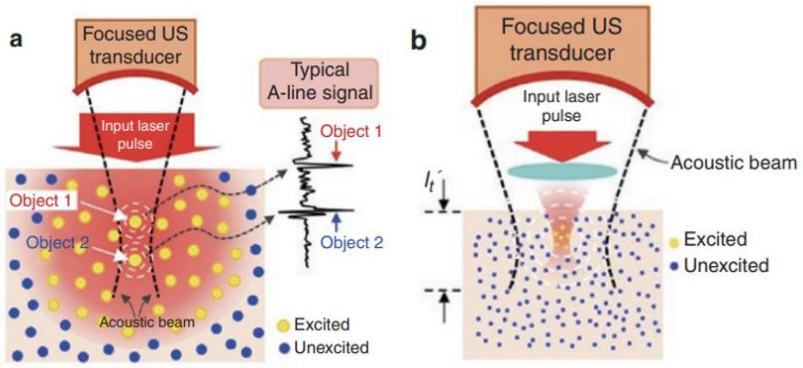

Figure 2: (a)Single-element focused transducer typically utilized in AR-PAM. (b) Single-element focused transducer typically utilized in OR-PAM [12].

The second method for detecting the photoacoustic signals is reserved for signals originating from shallow regions, called ballistic regions (TMFP less than ~ 1 mm). In this method, the photoacoustic waves are induced within the focal spot of the laser beam (Fig. 2(b)). This can be accomplished by appropriately adjusting the pulse energy. In this case, lateral resolution is determined by the beam diameter of the optical focus and not the acoustic beam diameter of the employed transducer. Optical parameters such as wavelength and optical numerical aperture (NA) play a role in determining the lateral resolution as well. This setup can achieve microscopy level lateral resolution [12].

Testing and Validation

The experiments that utilize photoacoustic tomography use various components such as endogenous and exogenous contrasts. Various chromophores such as melanin, oxygenated and deoxygenated hemoglobin molecules, have rich absorption variance which makes the PAT imaging procedure one of the most desirable procedures to acquire accurate data (Fig. 3).

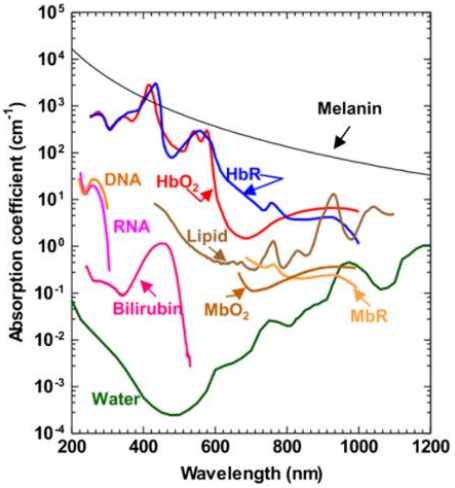

Figure 3 : PAT imaging of endogenous contrast agents, DNA/RNA, hemoglobin, and melanin [12].

PAT consists of multiple subdivisions which depend on the imaging depth that one is interested in. These subdivisions are Optical-Resolution Photoacoustic Microscopy (OR-PAM), Acoustic-Resolution Photoacoustic Microscopy (AR-PAM), Photoacoustic Computed Tomography (PACT), and Photoacoustic Endoscopy (PAE). Brain imaging procedures mainly utilize the AR-PAM and PACT due to the imaging depth opportunities.

AR-PAM involves the use of higher laser energy to be able to reach deeper into the organ of interest. It covers the quasi-diffusive imaging dept of the brain which is more than one transport mean free path (TMFP) bigger than one but less than 10 TMFP [14].This approach has been approved by the ANSI laser safety standards and the illumination of the AR-PAM can be either in a dark or bright field.

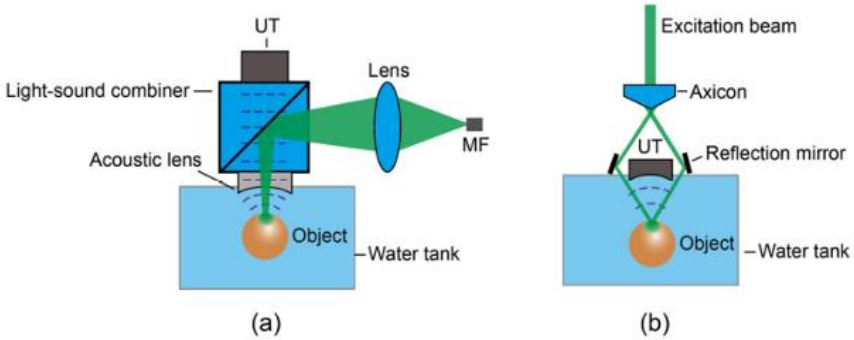

Figure 4 : Experimental setups for the AR-PAM under (a) bright field and (b) dark field illumination [8].

Bright field illumination can deliver higher optical fluence to the targeted volume, dark field illumination, on the other hand, can reduce surface interference for photoacoustic signals to penetrate deeper [8].

To achieve the desired spatial resolution of the AR-PAM using focused ultrasonic transducer with aperture of diameter D and focal length l, the following model can be used:

$$R_{lateral} = 0.71 * \lambda_0 * \frac{l}{\frac{D}{2}}$$

In the above equation, λ_o is the acoustic wavelength and D is the diameter of the transducer's aperture. The axial resolution that is desired to achieve can be acquired using following model :

$$R_{axial} = 0.88 * \frac{v_s}{B}$$

In the above equation, v_s is the speed of sound and B is the bandwidth of the ultrasonic transducer [8]. Bandwidth value depends on the desired imaging depth. It can be concluded that the imaging depth of interest using AR-PAM can be achieved by scaling the image resolution which depends on the central frequency and bandwidth of the ultrasonic transducer.

Another promising technique that has been utilized for brain imaging is Photoacoustic Computed Tomography (PACT). This technique uses an array of ultrasonic transducers to record the incoming photoacoustic waves from multiple view angles. This improves the speed of data acquisition but at the cost of the system expense and computational costs [8]. The PACT system has been observed to achieve a lateral resolution of 200 microns with the data acquisition rate of 8 frames/second [4].

In the experiment performed by Wang et al, adult Sprague-Dawley rats' hair was shaved, and the rats were anesthetized to keep them motionless. Then, rats were submerged in water and their mouths and noses were covered in aerophore to allow them to breathe. The thickness of their brain was recorded to be about 0.6-0.8 mm [9]. The laser light was shone on the area of interest and the data was collected. Afterwards, the rats were killed, and the open skull data collection was performed.

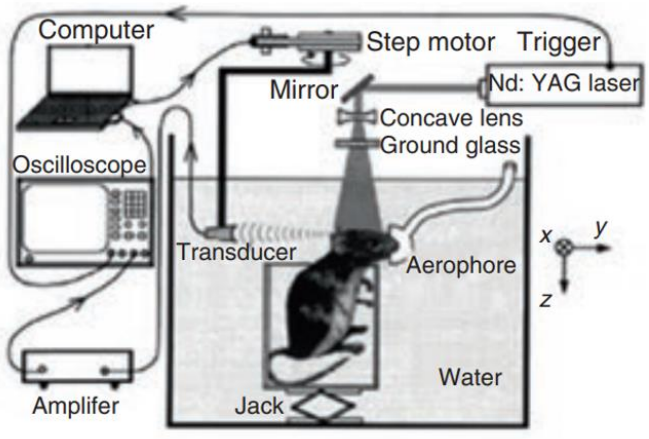

Figure 5 : Schematic showing the experimental setup by Wang, Pang et al.

The whisker stimulation of the experiment included simultaneously deflecting all whiskers on one side of the snout with a relay driven by a computer-controlled function generator. The researchers report that "the whiskers were deflected at 10Hz with an oscillation amplitude of ~8 mm at a distance of ~10 mm from the whisker pad, the whisker was stimulated for 4.5 seconds, and the photoacoustic signal was acquired during the 0.5-4.5 seconds after the start [9].

The optical absorption A(r) has been measured using the following model:

$$A(r) = -\frac{r_0^2 * C_p}{2 * \pi * v_s^4 * \beta} * \int_{\theta_0} d\theta_0 \frac{\partial p(r_0, t)}{t \partial t} \Big|_{t=\frac{r_0 - r}{v_s}}$$

In the brain imaging, oxygenated and deoxygenated oxygen values are crucial in obtaining functional information of the structure because these molecules have different absorption spectra μ_a (λ). The following oxygen saturation of hemoglobin (sO2) model is utilized for analysis:

$$sO_2 = \frac{C_{HbO_2}}{C_{HbO_2} + C_{HHb}}$$

The above equation stands for concentration of the oxygenated hemoglobin and stands for the deoxygenated hemoglobin concentration [7].

Results

From this study noninvasive PAT images were acquired when the mouse was alive as well as invasive images were collected using PAT.

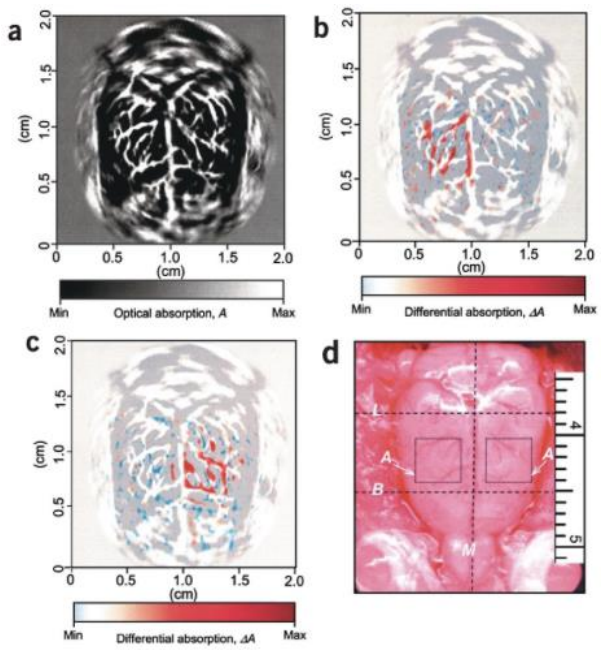

Figure 6: (a)Noninvasive PAT image of the vascular pattern in the superficial layer of the rat cortex, (b,c) Noninvasive functional PAT images of the left and right whisker stimulation, (d) Open skull photography of the rat cortical surface [9].

The fractional optical absorption in the large blood vessels within the activated regions was recorded to be ~8%. The changing of the hyperoxia statement to hypoxia statement induced significant increase in cerebral blood flow. Multiple experiments have been performed by many researchers to achieve the golden combination of high imaging depth and excellent spatial resolution. It has been stated in the paper by Wang and Maslov, a 44 µm lateral resolution was measured at a depth of 4.8 mm with a 50 MHz ultrasonic transducer. In another paper by Song and Wang, a lateral resolution of 560 µm was reported at a depth of 38 mm by using a 5 MHz ultrasonic transducer. In the experiment performed by Xia and Chatni, various organs of the mouse were imaged using PACT system that utilized a full-ring transducer array of 512 elements.

Limitations

The current PAT systems that are available are relatively bulky and can only be used on an optical table to image anesthetized animals. However, a recent study shows the development of a wearable PAM for brain imaging.

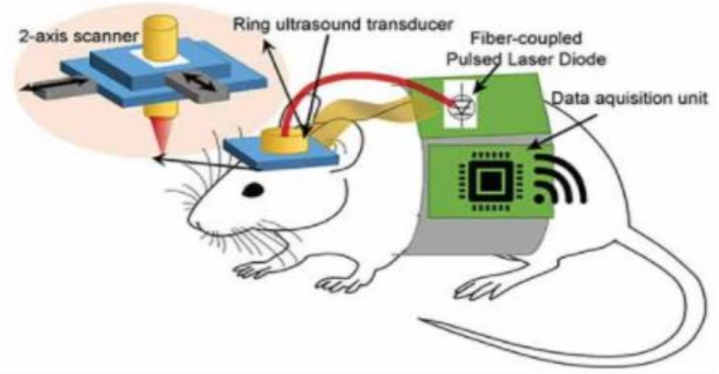

Figure 7: Schematic showing a wearable PAM for mouse brain imaging [1].

There is also a need to minimize the acoustic distortion from the skull as the skull and bone cavities may severely degrade the deep brain imaging quality, in order to address this issue, the bone profile will need to be mapped through another modality such as ultrasound computed tomography and then be incorporated into PAT reconstruction.

The major obstacle for imaging of the brain with PAT is the incident light and the emitted ultrasound needs to go through the thick human skull, which is approximately 7 to 11mm for adults, this is much thicker that the mouse skull which is approximately 0.2 to 0.3 mm.

The skull also introduces severe acoustic signal aberration that is associated with acoustic wave reflection and refraction within the skull. The acoustic aberration is a result of the acoustic impedance mismatch between the skull and the brain, the distorted acoustic waves can significantly deteriorate the reconstructed image.

Conclusion

PAT is a highly scalable imaging modality that is a promising tool for brain imaging, these advantages include rich selection of endogenous contrast, improved imaging depth, resolution, imaging speed and safety. It is inexpensive compared to other imaging modalities such as MRI and it provides superior penetration. Endogenous contrast enhancement reagents in PAI will become increasingly important for monitoring neural activity, glucose uptake, aberrant protein aggregation, malignancy, and deep brain tumors.

References

[1] Nie, L., Cai, X., Maslov, K., Garcia-Uribe, A., Anastasio, M. A., & Wang, L. V. (2012). Photoacoustic tomography through a whole adult human skull with a photon recycler. Journal of Biomedical Optics, 17(11), 110506. https://doi.org/10.1117/1.JBO.17.11.110506

[2] Ovsepian, S. V., Olefir, I., Westmeyer, G., Razansky, D., & Ntziachristos, V. (2017a). Pushing the boundaries of neuroimaging with optoacoustics. Neuron, 96(5), 966–988. https://doi.org/10.1016/j.neuron.2017.10.022

[3] Ovsepian, S. V., Olefir, I., Westmeyer, G., Razansky, D., & Ntziachristos, V. (2017b). Pushing the boundaries of neuroimaging with optoacoustics. Neuron, 96(5), 966–988. https://doi.org/10.1016/j.neuron.2017.10.022

Song, K. H., & Wang, L. V. (2007). Deep reflection-mode photoacoustic imaging of biological tissue. Journal of Biomedical

[4] Optics, 12(6), 060503. https://doi.org/10.1117/1.2818045

[5] Wang, D., Wu, Y., & Xia, J. (2016). Review on photoacoustic imaging of the brain using nanoprobes. Neurophotonics, 3(1), 010901. https://doi.org/10.1117/1.NPh.3.1.010901

[6] Wang, L. V. (Ed.). (2017). Photoacoustic imaging and spectroscopy (1st ed.). CRC Press. https://doi.org/10.1201/9781420059922

[7] Wang, L. V., & Gao, L. (2014a). Photoacoustic microscopy and computed tomography: From bench to bedside. Annual Review of Biomedical Engineering, 16, 155–185. https://doi.org/10.1146/annurev-bioeng-071813-104553

[8] Wang, L. V., & Gao, L. (2014b). Photoacoustic microscopy and computed tomography: From bench to bedside. Annual Review of Biomedical Engineering, 16(1), 155–185. https://doi.org/10.1146/annurev-bioeng-071813-104553

[9] Wang, X., Pang, Y., Ku, G., Xie, X., Stoica, G., & Wang, L. V. (2003a). Noninvasive laser-induced photoacoustic tomography for structural and functional in vivo imaging of the brain. Nature Biotechnology, 21(7), 803–806. https://doi.org/10.1038/nbt839

[10] Xia, J., Yao, J., & Wang, L. V. (2014). Photoacoustic tomography: Principles and advances. Electromagnetic Waves (Cambridge, Mass.), 147, 1–22. https://www.ncbi.nlm.nih.gov/pmc/articles/PMC4311576/

[11] Yang, J.-M., & Ghim, C.-M. (2021a). Photoacoustic tomography opening new paradigms in biomedical imaging. Advances in Experimental Medicine and Biology, 1310, 239–341. https://doi.org/10.1007/978-981-33-6064-8_11

[12] Yang, J.-M., & Ghim, C.-M. (2021b). Photoacoustic tomography opening new paradigms in biomedical imaging. Advances in Experimental Medicine and Biology, 1310, 239–341. https://doi.org/10.1007/978-981-33-6064-8_11

[13] Yang, J.-M., & Ghim, C.-M. (2021c). Photoacoustic tomography opening new paradigms in biomedical imaging. In J. K. Kim, J. K. Kim, & C.-G. Pack (Eds.), Advanced Imaging and Bio Techniques for Convergence Science (Vol. 1310, pp. 239–341). Springer Singapore. https://doi.org/10.1007/978-981-33-6064-8_11

[14] Yao, J., & Wang, L. V. (2014a). Photoacoustic brain imaging: From microscopic to macroscopic scales. Neurophotonics, 1(1), 1877516. https://doi.org/10.1117/1.NPh.1.1.011003

[15] Yao, J., & Wang, L. V. (2014b). Photoacoustic brain imaging: From microscopic to macroscopic scales. Neurophotonics, 1(1), 011003. https://doi.org/10.1117/1.NPh.1.1.011003

[16] Zhao, Z., & Myllylä, T. (2021). Recent technical progression in photoacoustic imaging—Towards using contrast agents and multimodal techniques. Applied Sciences, 11(21), 9804. https://doi.org/10.3390/app11219804

[17] Zhou, Y., Yao, J., & Wang, L. V. (2016a). Tutorial on photoacoustic tomography. Journal of Biomedical Optics, 21(6), 061007. https://doi.org/10.1117/1.JBO.21.6.061007

[18] Zhou, Y., Yao, J., & Wang, L. V. (2016b). Tutorial on photoacoustic tomography. Journal of Biomedical Optics, 21(6), 061007. https://doi.org/10.1117/1.JBO.21.6.061007